

Article

The Non-Uniformity Control Strategy of a Marine High-Speed Diesel Engine Based on Each Cylinder's Exhaust Temperature

Liangtao Xie , Sicong Sun  and Fei Dong 

School of Naval Architecture, Ocean and Energy Power Engineering, Wuhan University of Technology, Wuhan 430063, China

* Correspondence: 216281@whut.edu.cn

Abstract: To improve the non-uniformity of a multi-cylinder marine diesel engine caused by manufacturing assembly errors and performance degradation of the fuel injection system, with the instantaneous speed applied as the control target, the feedback variable of each cylinder's exhaust temperature was used to obtain the non-uniformity information and the injection quantity of each cylinder was applied as the control variable; the inhomogeneity control was accomplished by modifying the injection pulse spectrum. The model of AVL Cruise M was established and validated by bench test data. The non-uniformity control strategy based on the instantaneous speed and the exhaust temperature of each cylinder was developed in SIMULINK, and the control effect was compared with the closed-loop control of cylinder pressure by software in-loop simulation. The results showed that the non-uniformity control strategy based on exhaust temperature could significantly improve the uniformity of each cylinder; although the improvement effect was not as great as the non-uniformity control strategy based on cylinder pressure, the cost was significantly reduced, and the practicality and reliability were better. With the closed-loop control of exhaust temperature and instantaneous speed, the CV (Coefficient of Variation) of IMEP (indicated effective pressure) was close to the closed-loop control of cylinder pressure; the maximum occurred at 25% load when it was 0.199%. This co-simulation provided a theoretical basis for the subsequent hardware-in-the-loop simulation and actual engine tests.



Citation: Xie, L.; Sun, S.; Dong, F. The Non-Uniformity Control Strategy of a Marine High-Speed Diesel Engine Based on Each Cylinder's Exhaust Temperature. *Processes* **2023**, *11*, 1068. <https://doi.org/10.3390/pr11041068>

Academic Editors: Leszek Chybowski, Jarosław Myśków, Przemysław Kowalak, Andrzej Jakubowski and Wen-Jer Chang

Received: 7 March 2023

Revised: 25 March 2023

Accepted: 30 March 2023

Published: 2 April 2023



Copyright: © 2023 by the authors. Licensee MDPI, Basel, Switzerland. This article is an open access article distributed under the terms and conditions of the Creative Commons Attribution (CC BY) license (<https://creativecommons.org/licenses/by/4.0/>).

Keywords: multi-cylinder marine diesel engine; non-uniformity control strategy; closed-loop control; exhaust temperature

1. Introduction

Marine diesel engines are widely used as power sources and generator sets for large ships with their advantages of high power, low fuel consumption rate, and high reliability [1–3]. Intelligence represents the development trend of marine diesel engines; traditional electronically controlled diesel engines are based on open-loop control test calibration data, and diesel engine processing and manufacturing process errors and the wear and aging of parts easily make the diesel engine work unevenly in each cylinder. As such, there is room for performance optimization [4–6]. Diesel engine inhomogeneity will intensify each cylinder's mechanical load and thermal load fluctuations, severely damaging the diesel engine.

The number of marine high-powered high-speed HPCR (high-pressure common rail) diesel engine cylinders can reach 20; because of variations in the production and manufacturing of electronically controlled injectors, the actual injection quantity of each cylinder with the same solenoid actuation signal is not consistent. Meanwhile, there may be installation errors such as eccentricity in the cam mechanism of the diesel engine, resulting in deviation angles in the TDC (top dead center) signal of each cylinder, thus affecting the consistency of the injection timing; ultimately, the actual combustion and working principle of each cylinder are different [7–9]. The CUC (Cylinder Uniformity Control) of

each cylinder is a basic requirement to ensure diesel engine operation remains steady, and is a key technology for the improvement of the overall performance of diesel engines [10–14]. Conventional diesel engine control systems are generally based on the test calibration data of the pulse spectrum for fuel injection control. The control parameters cannot be modified in response to the changes in the operating conditions of a single cylinder.

At present, the research on the non-uniformity of each cylinder mainly focuses on the instantaneous speed and cylinder pressure [14–16]. Zheng used the burst pressure, the IMEP, and the exhaust temperature of each cylinder as control variables to correct the gas injection pulse width of each cylinder for the multi-cylinder unbalance problem of marine micro-ignition dual-fuel engines. The burst pressure equilibrium was less than 1.2%, the IMEP equilibrium was less than 0.8%, and the exhaust temperature equilibrium was within 11 °C [17]. Ou proposed an anomaly identification and reconstruction method for combustion analysis systems. The effectiveness of the anomaly identification and reconstruction algorithm in locating the abnormal cylinder pressure on a crank-angle basis, and in reconstructing the cylinder pressure by rejecting measurement noise without losing valuable sensing information was determined [18]. Yu performed a study of the combustion stability and uniformity of marine low-speed and medium-speed diesel engines; a closed-loop control strategy for cylinder pressure was developed, and the in-cylinder combustion state indicators such as the IMEP and MFB50 (50% of the mass fraction burned) were calculated to adjust the injection parameters, which had an improvement effect on the combustion imbalance between each cylinder and cycle [19,20]. Yang presented a dynamic model for simulating the instantaneous angular speed, and the instantaneous angular speed waveforms both in the fuel leakage condition and in the normal condition were measured under various engine speeds and loads in laboratory conditions. The characteristic parameters for detecting the faults relating to the gas pressure in the cylinder were obtained successfully [21]. Wang used a TBD314V8 diesel engine as a research object to improve the unevenness of each cylinder. The IMEP and MFB50 of each cylinder based on the cylinder pressure calculation were used as the feedback variables, and the injection quantity and injection advance angle of each cylinder were used as the control variables to establish a joint simulation model of GT-Power and Simulink [5].

The closed-loop control technique based on cylinder pressure is not suitable for multi-cylinder diesel engines because of the high cost of cylinder pressure sensors and the large amount required [14]. The cylinder uniformity control of marine diesel engines based on exhaust temperature has the advantages of low-cost sensors, straightforward operation, and suitability for long-term online measurement, despite the disadvantage of at least one operating cycle deferral. Moreover, the in-cylinder method is more accurate than the exhaust temperature method; the in-cylinder method is therefore suitable for engines with fewer cylinders. The CUC of diesel engines based on instantaneous speed has the advantages of economic performance, straightforward operation, and suitability for long-term online measurement, therein being able to monitor and diagnose the condition of each cylinder in real time [15]. Currently, this method is mainly applied to diesel engines with small numbers of cylinders and large firing interval angles. For multi-cylinder diesel engines with overlapping firing intervals and bad work balances, the general waveform characteristic parameters cannot easily be used to perform an accurate diagnosis of the extent of the fault and the location of the faulty cylinder because of the strong inter-cylinder coupling [22].

Exhaust temperature sensors are applied in the CUC of marine diesel engines because of their easy installation and low price, despite the disadvantage of at least one operating cycle deferral. To improve the uniformity of each cylinder caused by the fuel injection system, a closed-loop control strategy based on the exhaust gas temperature was adopted to improve the uniformity of each cylinder caused by the fuel injection system. The effect of the uniformity control strategy of each cylinder and the overall performance of the marine high-speed diesel engine was investigated, providing a theoretical basis for hardware-in-the-loop simulation and real engine tests. Combining the characteristics of

instantaneous speed with exhaust temperature in the CUC, the instantaneous speed and exhaust temperature of each cylinder were utilized to control non-uniformity. By measuring the instantaneous angular acceleration of each cylinder in a cycle, the operating differences between cylinders can be determined. If this variation was out of range, the pulse spectrum was modified by a strategy that combines the magnitude of the variation with the exhaust temperature to modify the fuel quantity so that the instantaneous speed was kept consistent. The exhaust temperature was utilized as a measure of non-uniformity for each cylinder, and the closed-loop control regulated the fuel injection quantity to complete the CUC.

2. Modeling and Verification

As illustrated in the software in-loop simulation process in Figure 1, the model mainly consists of modules such as the diesel engine block, turbocharger, fuel system, and gas-exchanging system. The CHD622V20 marine high-speed engine was studied and a real-time simulation model was established in AVL Cruise M. The accuracy and real-time of the model were verified by bench test data. A CUC strategy based on the instantaneous speed and exhaust temperature of each cylinder was developed in SIMULINK, and the marine high-speed engine model was integrated into the loop. The CUC of the marine high-speed diesel engine was investigated and compared with the cylinder-pressure-based control strategy to provide a theoretical basis for subsequent hardware-in-the-loop and tests.

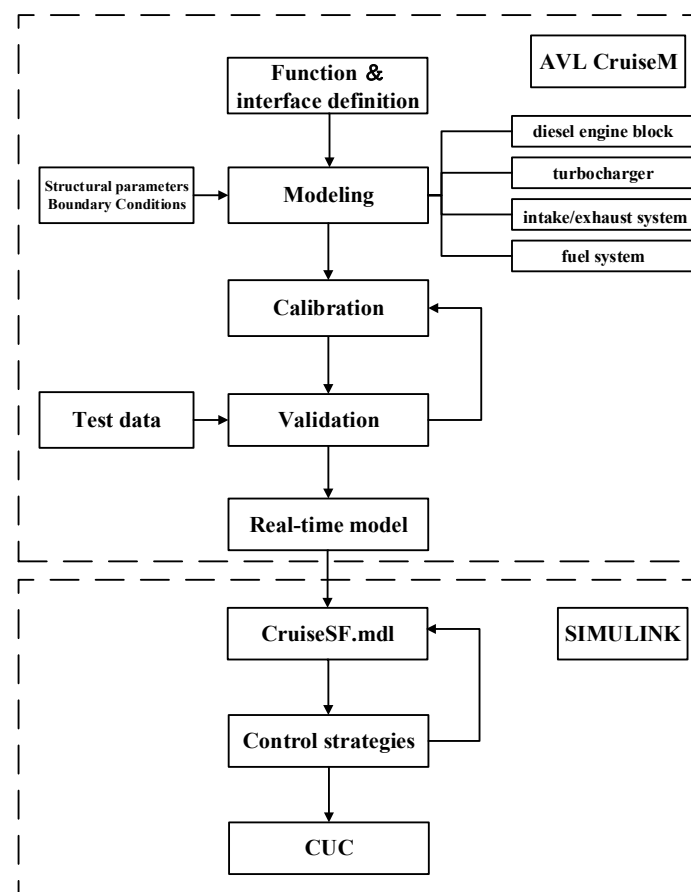


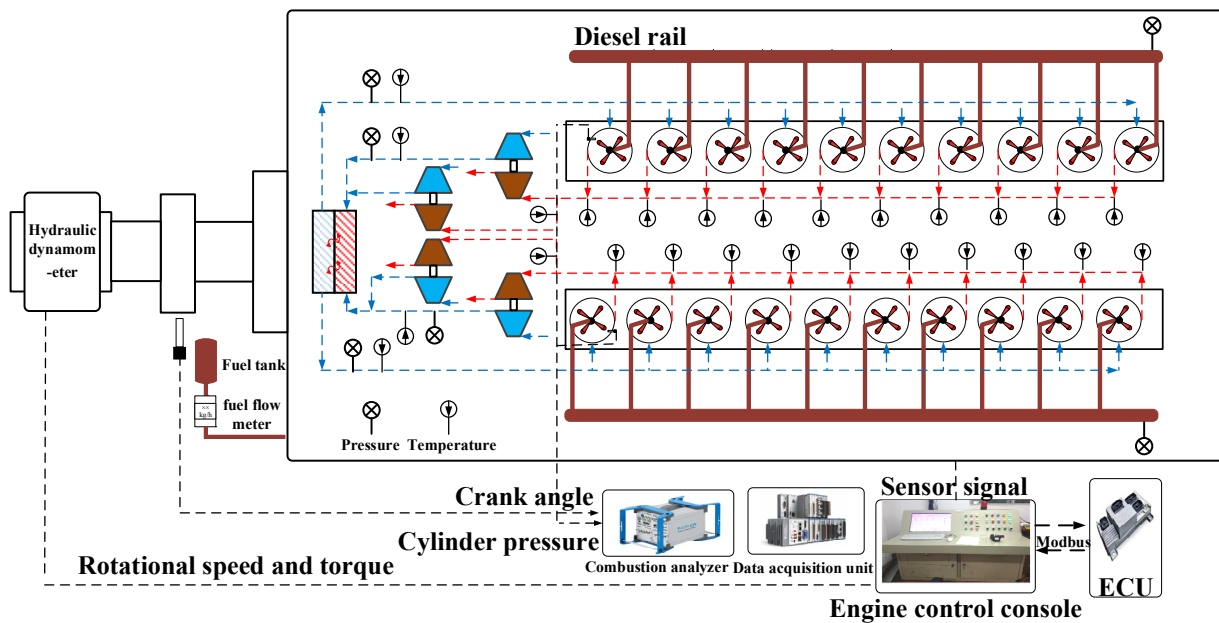
Figure 1. Software in-loop simulation process.

2.1. The Test Benches

The basic technical parameters of the CHD622V20 high-speed marine engine (high-speed engine) are shown in Table 1. The layout of the CHD622V20 test bench is shown in Figure 2.

Table 1. The basic technical parameters of the high-speed engine.

Project	Parameter
Bore/(mm)	170
stroke/(mm)	215
Number of cylinders	20
Compression ratio	15
Rated speed/(r/min)	1500
Power rating/(kW)	3600
Type of fuel system	HPCR
Firing order	A1-B7-A2-B5-A4-B3-A6-B1-A8-B2-A10-B4-A9-B6-A7-B8-A5-B10-A3-B9

**Figure 2.** The CHD622V20 test bench layout.

2.2. Modeling

2.2.1. Heat Transfer Model

To calculate the heat between the working medium in the cylinder and the thermal system boundary, radiation heat transfer is usually neglected, the working medium in the cylinder is regarded as a uniform field, and an empirical formula is used to establish a heat conduction model.

$$Q_{wi} = A_i \alpha_w (T_c - T_{wi}) \quad (1)$$

where Q_{wi} is the heat between the working substance and the thermal system boundary (J); A_i is the surface area of the thermal system boundary (m^2); α_w is the heat transfer coefficient ($W/m^2 \cdot K$); T_c is the working substance temperature in the cylinder ($^{\circ}C$); and T_{wi} is the temperature of the thermal system boundary ($^{\circ}C$).

2.2.2. MCC (Mixing Controlled Combustion) Model

An MCC combustion model was utilized to simulate the in-cylinder combustion process of a diesel engine. The model can predict the combustion and heat release of a diesel engine based on the changes in the injection parameters and the simulated gas exchange process calculated in real time by the fuel injection model [23].

The MCC model divides the cylinder into two regions: premixed combustion and diffusion combustion, and the reaction rate in the premixed combustion stage was calculated by Equation (2).

$$\frac{dQ_{pre}}{dt} = C_{pre} \cdot \lambda \cdot AF_{ST} \cdot \frac{m_{f,pre}}{V_{mix}} \cdot H_u \cdot e^{-\frac{\kappa T_A}{T_c}} \cdot (t - t_{ign})^2 \quad (2)$$

where Q_{pre} is the heat in the premixed combustion (J); C_{pre} is the premixed combustion exothermic calibration parameter (-); λ is the excess air coefficient (-); AF_{ST} is the stoichiometric air/fuel ratio (-); $m_{f,pre}$ is the fuel mass in the premixed (kg); V_{mix} is the fuel injection volume (m^3); H_u is the low heating value of the fuel (J/kg); κ and T_A are the Arrhenius exothermic model constants (-); and $t - t_{ign}$ is the length of time since fuel ignition (s).

The diffusion combustion stage considers the wall effect and the effect of EGR on combustion, as shown in Equation (3).

$$\frac{dQ_{diff}}{dt} = C_{comb} \cdot F_{wall} \cdot F_{egr} \cdot H_u \cdot m_{f,diff,net} \cdot \frac{\sqrt{k}}{\sqrt[3]{V_c}} \quad (3)$$

where Q_{diff} is the heat in the diffusion combustion (J); C_{comb} is calibrated experimentally and related to speed (-); F_{wall} is the function of wall effects during fuel injection; F_{egr} is the function of residual gas effects; $m_{f,diff,net}$ is the fuel mass during the diffusion combustion (kg); k is the turbulent kinetic energy intensity (J); and V_c is the cylinder volume (m^3).

2.2.3. Intake and Exhaust System Model

$$\frac{d(m_c \cdot u)}{d\alpha} = -p_c \cdot \frac{dV_{cyl}}{d\alpha} - \Sigma \frac{dQ_w}{d\alpha} + \Sigma \frac{dm_i}{d\alpha} \cdot h_i - \Sigma \frac{dm_e}{d\alpha} \cdot h_e \quad (4)$$

where m_c is the quality of the working substance in the cylinder (kg); u is the ratio of the internal energy (J), P_c is the pressure in the cylinder (MPa), Q_w is the heat transfer rate (J), dm_i is the quality of the air flowing into the cylinder (kg/s), dm_e is the quality of the exhaust gas flowing (kg/s), h_i is the inflow enthalpy (kJ/kg), and h_e is the outflow enthalpy (kJ/kg).

$$T_s = \frac{T_K - T_{wo}}{\exp \left[C_{sw} \cdot (T_K - T_s + T_{wi} - T_{wo}) / \frac{dm_w}{dt} \cdot c_{pw} \cdot (T_{wo} - T_{wi}) \right]} + T_{wi} \quad (5)$$

$$T_{wo} = T_{wi} + \left(\frac{dm_s}{dt} \cdot c_{ps} / \frac{dm_w}{dt} \cdot c_{pw} \right) \cdot (T_k - T_s) \quad (6)$$

where T_K is the temperature of the air before intercooling ($^{\circ}C$), T_s is the temperature of the air after intercooling ($^{\circ}C$), and T_{wo} is the temperature of the coolant after intercooling ($^{\circ}C$). According to the principle of energy conservation, the heat lost by the compressed air dQ_s/dt , the heat gained by the coolant dQ_w/dt , and the heat transferred from the compressed air to the coolant dQ_{sw}/dt are equal, thus deriving the formula for the temperature of the cooled, compressed air and the coolant at the outlet.

2.2.4. Fuel Injection Model

$$\frac{dP_{rail}}{dt} = \frac{E}{V_{rail}} \cdot \frac{1}{\rho_{rail}} \cdot \left(\frac{dm_{pump}}{dt} + \frac{dm_{inj}}{dt} \right) \quad (7)$$

where P_{rail} is the pressure in the common rail (MPa); E is the volume elastic modulus of the fuel (MPa); V_{rail} is the volume of the common rail (m^3); ρ_{rail} is the density of the liquid

fuel in the common rail (kg/m^3); dm_{pump} is the fuel mass supplied to the high-pressure oil pump (kg/s); and dm_{inj} is the fuel mass supplied to the common rail injector (kg/s).

$$\frac{dm_{inj}}{dt} = \sqrt{2 \cdot \rho_{fuel} \cdot (P_{pipe} - P_c) \cdot (\zeta_{NS}/A_{NS}^2 + \zeta_{NH}/A_{NH}^2)^{-1}} \quad (8)$$

where ρ_{fuel} is the density of fuel (kg/m^3); P_{pipe} is the pressure in the high-pressure oil pipe (MPa); ζ_{NS} is the flow coefficient of the needle valve seat; A_{NS} is the flow cross-sectional area of the needle valve seat (m^2); ζ_{NH} is the flow coefficient of the nozzle; and A_{NH} is the cross-sectional flow area of the nozzle hole (m^2).

2.2.5. AVL CRUISE M Model

As shown in Figure 3, the CHD622V20 marine high-speed engine real-time model was established in AVL Cruise M. The model mainly consists of modules such as the heat transfer, MCC, exhaust, and fuel injection.

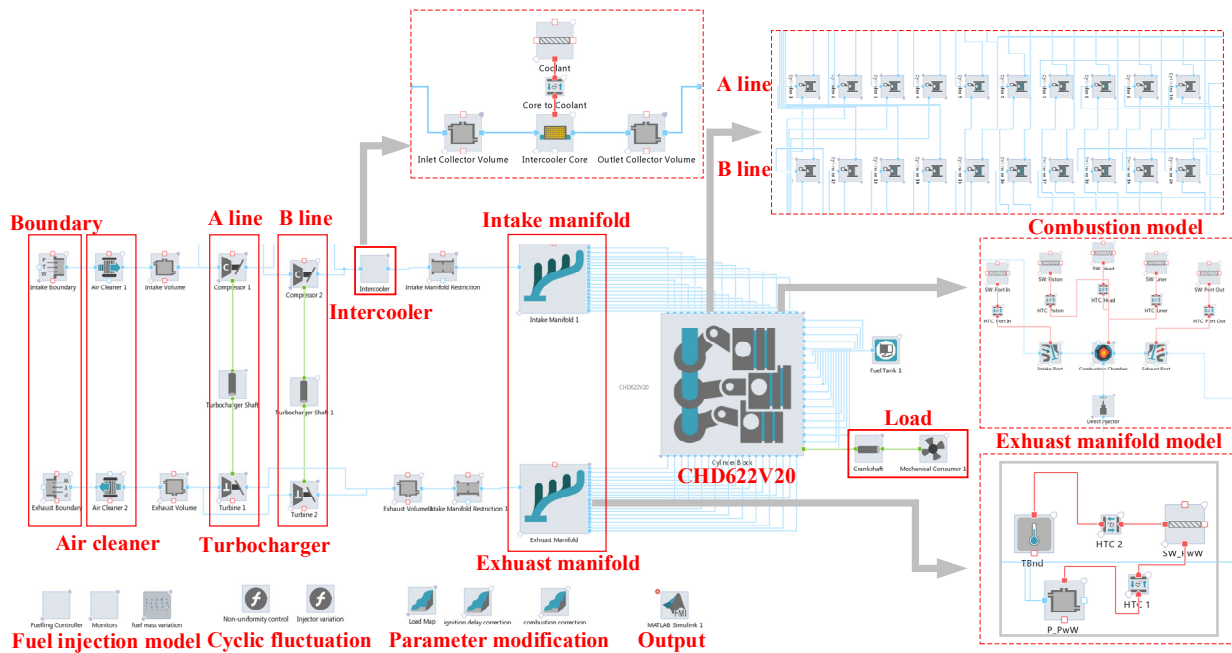


Figure 3. The CHD622V20 model.

2.2.6. Simulation of Cyclic Fluctuations

As the combustion parameters of the diesel engine obey Gaussian distribution [24], the Marsaglia–Bray algorithm was applied to Gaussian distribution on the boundary conditions [25], mainly including the fuel injection and gas exchange processes which have an impact on the combustion state, simulating its random fluctuation process during the operation of the diesel engine. The calculation steps are as follows:

- (1) Generate two independent, identically distributed $U(0, 1)$ random numbers U_1 and U_2 ;
- (2) $V_i = 2U_i - 1 (i = 1, 2), S = V_1^2 + V_2^2$;
- (3) If $S > 1$, return to step (1); conversely, calculate $Y = \sqrt{((-2)\ln S/S)}$, output $X_1 = V_1 Y$.

A pair of mutually independent random sequences of standard normal distribution can be obtained using this algorithm [26]. The algorithm is faster in calculation, simpler in programming language, and requires less storage space, thereby meeting the real-time requirements of the real-time model of the marine high-speed engine. The exhaust temperature of each cylinder is shown in Figure 4. The high-speed engine was simulated with large cyclic fluctuations under different loads.

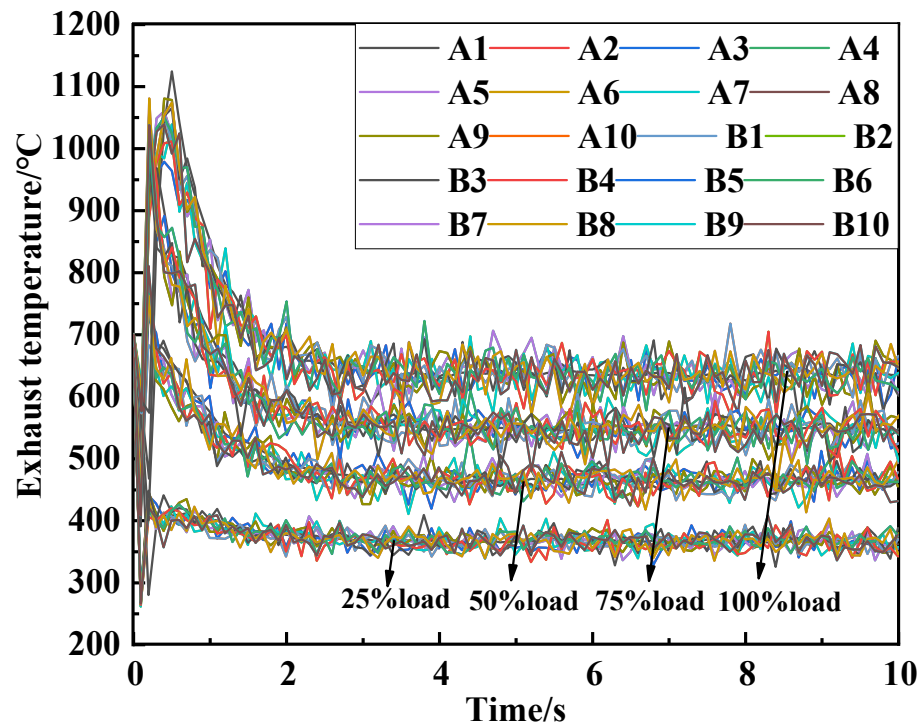


Figure 4. The simulation of the exhaust temperature fluctuation of the engine.

2.3. Real-Time Model Verification

Figure 5 shows the comparison between the simulated and the tested cylinder pressure at rated speeds and different loads. Except for the test data in the low-pressure part, which have some measurement errors because of the limitation of the sensor, the maximum error between the simulation data and the test data in the high-pressure part did not exceed 5%; therefore, the real-time model can better reflect the performance of the diesel engine.

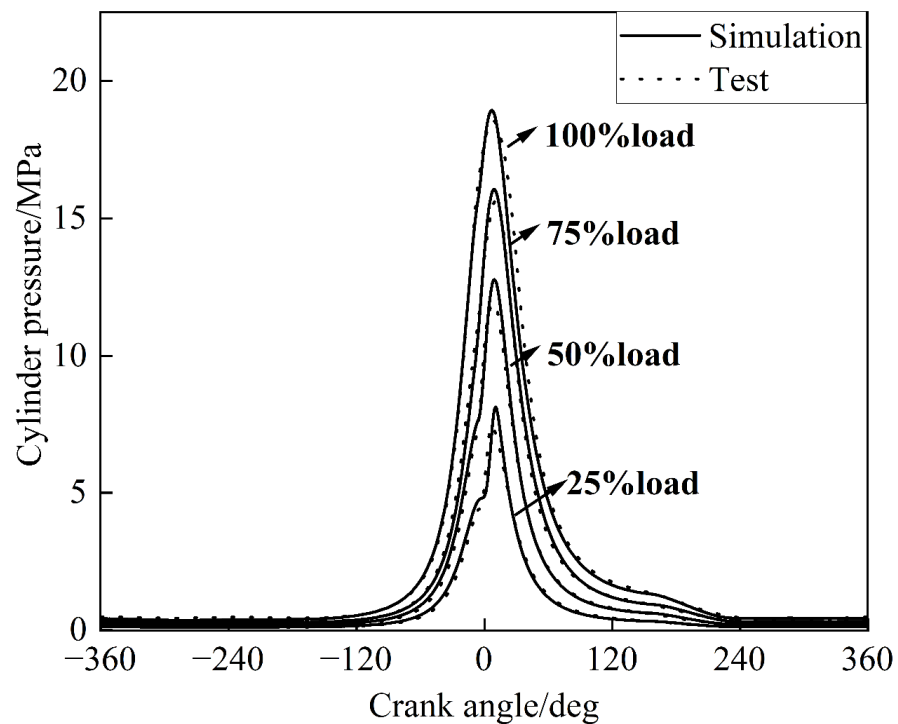


Figure 5. Comparison of cylinder pressure verification under different loads.

Figure 6 shows the cylinder pressure curves of twenty cylinders in a high-speed engine under 100% load, and Figure 7 shows the cylinder pressure curves of different cycles of the A1 cylinder under 100% load.

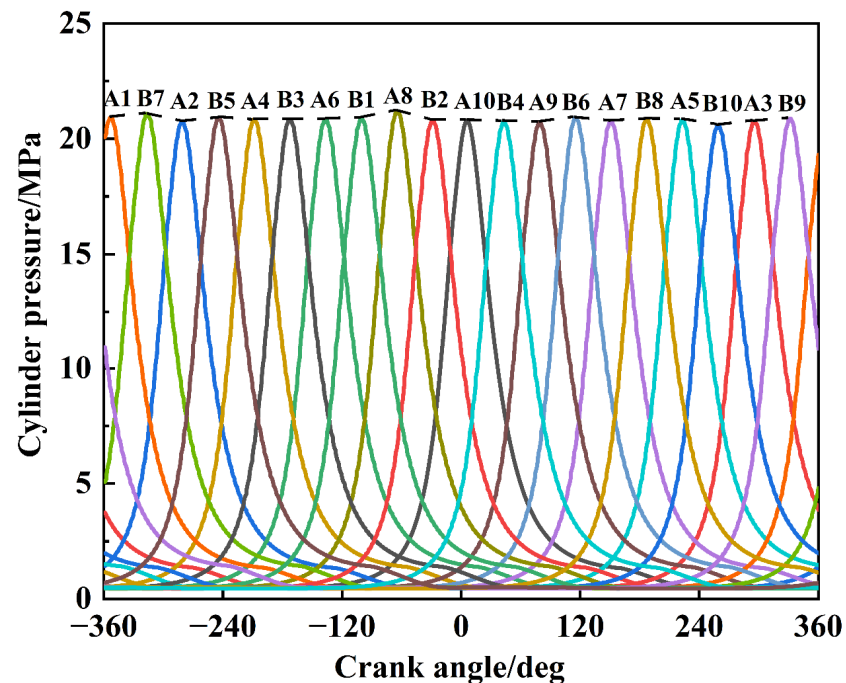


Figure 6. The pressure of twenty cylinders.

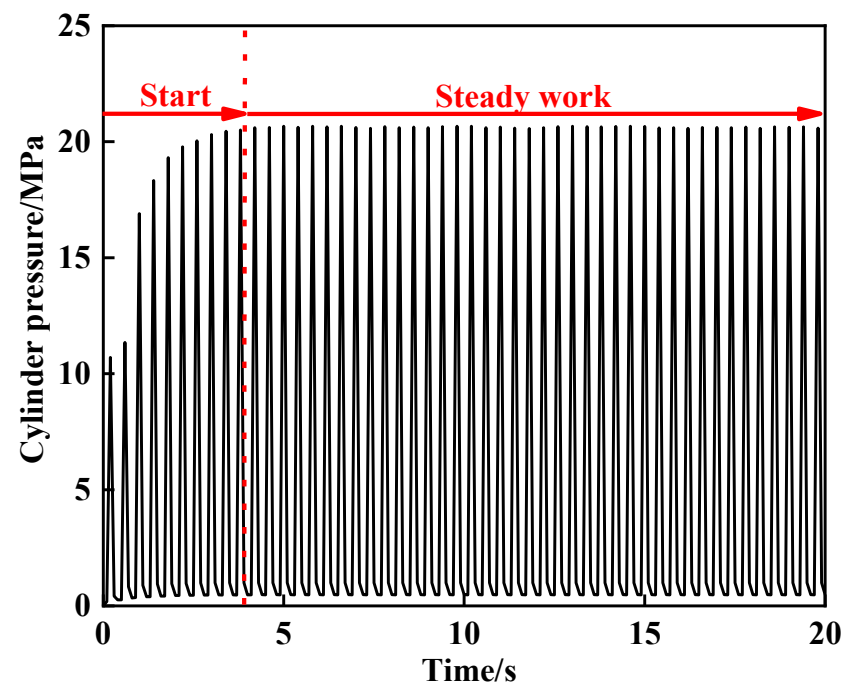


Figure 7. The pressure of the A1 cylinder.

Figure 8 shows a comparison of the IMEP and output power for the high-speed engine. The error between the IMEP and output power was within 5% for each load, with the maximum error occurring at 25% of the operating conditions, i.e., 4.90% for IMEP and 2.37% for output power. The mean error between the simulation and test IMEP was 3.01%, and the mean error between the simulation and test output was 1.79%.

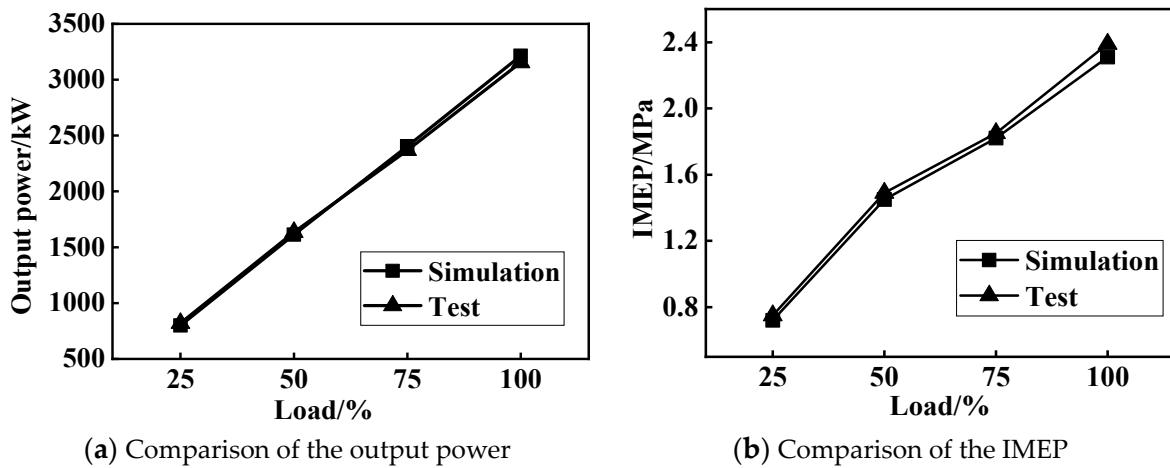


Figure 8. The comparison of the IMEP and output power for the high-speed engine.

Figure 9 shows the comparison between the simulation data and the test data of exhaust temperature (T_{ex}) of each cylinder. Figure 10 shows the comparison between the simulation data and the test data for each load of the high-speed engine. The error between the simulation data and the test data for each load was within 5%, and the maximum error was 4.20%, which occurred at 100% working condition.

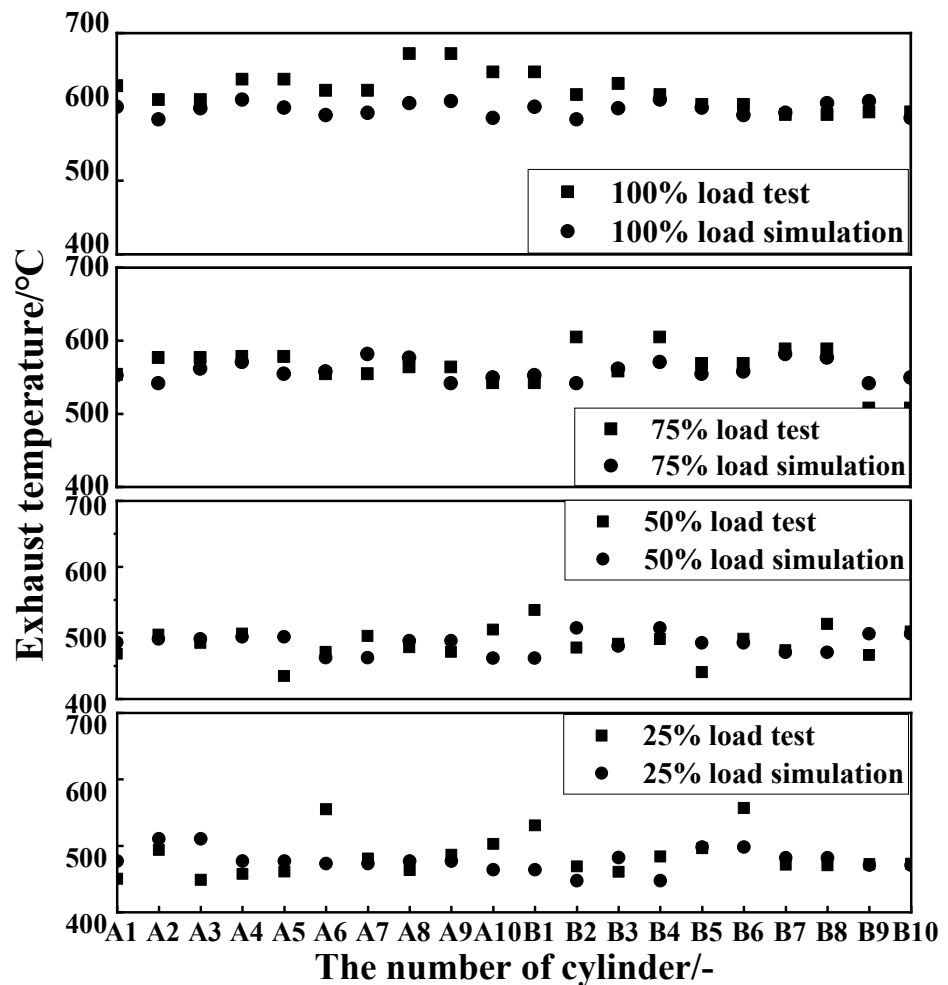


Figure 9. Comparison of T_{ex} simulation and test.

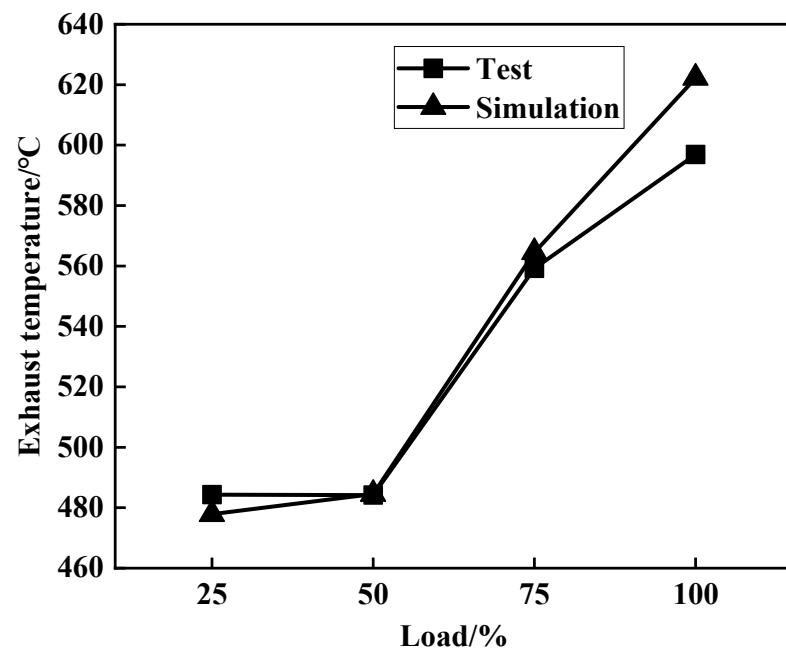


Figure 10. Comparison of T_{ex} for each load.

The high-speed engine model needs to operate in real-time while ensuring computational accuracy to meet the commissioning needs of the inhomogeneity control strategy. The real-time factor can be used as a criterion to determine the real-time performance of the model. When the real-time factor is less than 1, it means that the diesel engine model calculates faster than the real diesel engine works. The real-time factor of the high-speed engine model at rated speed is shown in Figure 11; with an Intel 3.2 GHz CPU (central processing unit) configuration, the maximum value of the real-time factor was 0.89 and the average value was 0.5825, both of which are less than 1, thereby meeting the requirements of debugging and verification of the inhomogeneity control strategy.

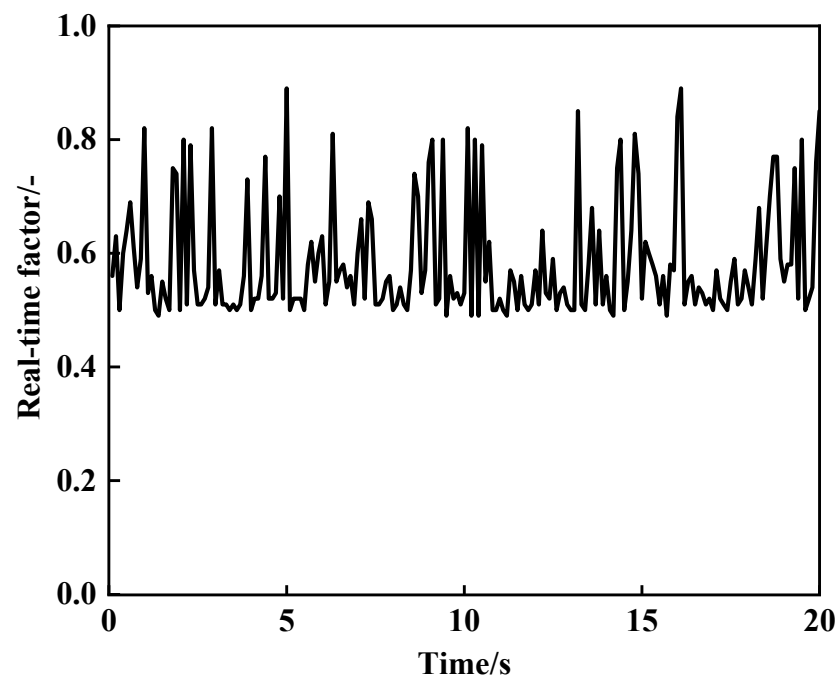


Figure 11. Real-time factors of the real-time model.

3. Non-Uniformity Control Strategy

3.1. Feedback Variable and Control Variable

The performance of each cylinder can be shown by the feedback variable in real time, which should be easily accessible, reliable, and accurate [27]. The fluctuating characteristics of instantaneous speed that depend on factors such as gas pressure and reciprocating inertia forces contain a wealth of information about the performance of each of the engine's cylinders. Exhaust temperature (T_{ex}) is an essential indicator of the multi-cylinder operation uniformity, which is utilized to visually detect abnormal combustion such as misfires and becomes a feedback variable for closed-loop combustion control. However, the exhaust temperature is a slow-varying and real-time signal and has a certain lag when used as a feedback variable. Hence, it needs to be combined with the instantaneous speed as the feedback variable for closed-loop control.

The injection quantity was taken as the control variable. The fuel injection quantity was adjusted by changing the injection pulse width to modify the work capacity of each cylinder, which in turn determined the exhaust temperature of each cylinder. The variation in operation between the cylinders could be obtained by measuring the instantaneous angular acceleration of each cylinder after one operating cycle [28]. The CV of the instantaneous angular acceleration, i.e., the ratio of the standard variation to the mean value, was utilized as the evaluation index. If the variation was unreasonably out of range, the base fuel quantity of each cylinder was corrected in the next cycle based on the size of the variation combined with the strategy of exhaust temperature so that the instantaneous speed of each cylinder converged.

The instantaneous speed was utilized as the evaluation index of the non-uniformity of the performance of each cylinder, the exhaust temperature signal of each cylinder was utilized as the feedback variable, and the injection quantity was used as the control variable of the non-uniformity control strategy. The strategy flow is shown in Figure 12.

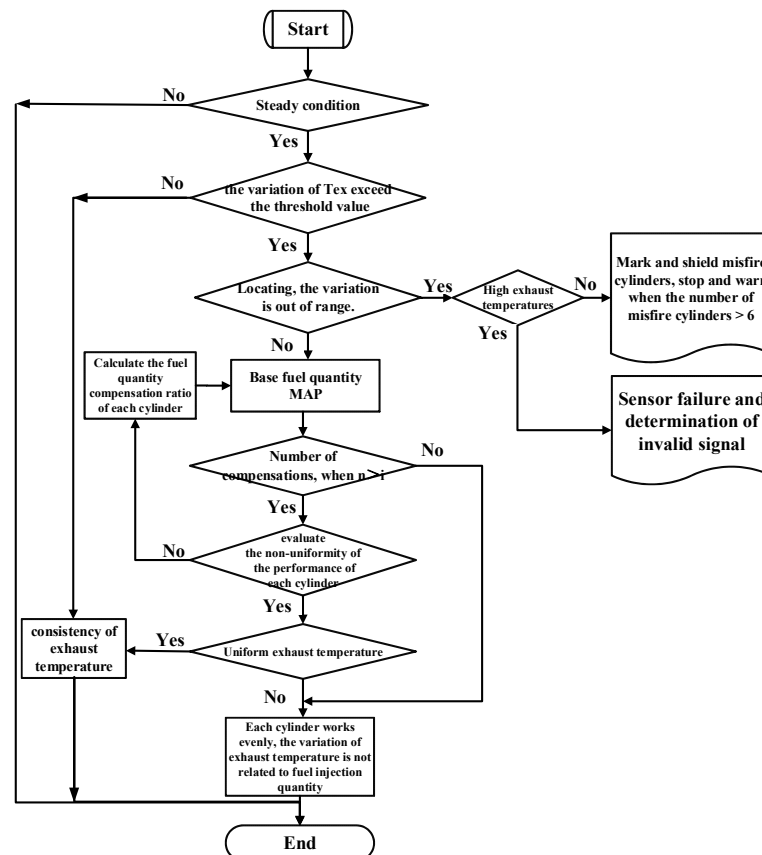


Figure 12. The flow of the CUC strategy.

3.2. Exhaust Temperature Signal Analysis

The instantaneous speed was taken as the control target in this control strategy. When performing the initial determination of instantaneous speed for diesel engines, the speed fluctuation rate should not exceed the speed regulation requirement of secondary accuracy. The instantaneous speed decision module is shown in Figure 13. The exhaust temperature was calibrated and analyzed to obtain information that can work as a feedback signal to reflect the non-uniformity of each cylinder. The exhaust temperature signal analysis was conducted as follows: the exhaust temperature signal validity was judged; the exhaust temperature rose slowly during the starting process, and could not be transient. In the validity judgment, the exhaust temperature was measured after a certain period. Signals that exceeded the range of the exhaust gas temperature sensor were judged as invalid signals by the sensor failure judgment module.

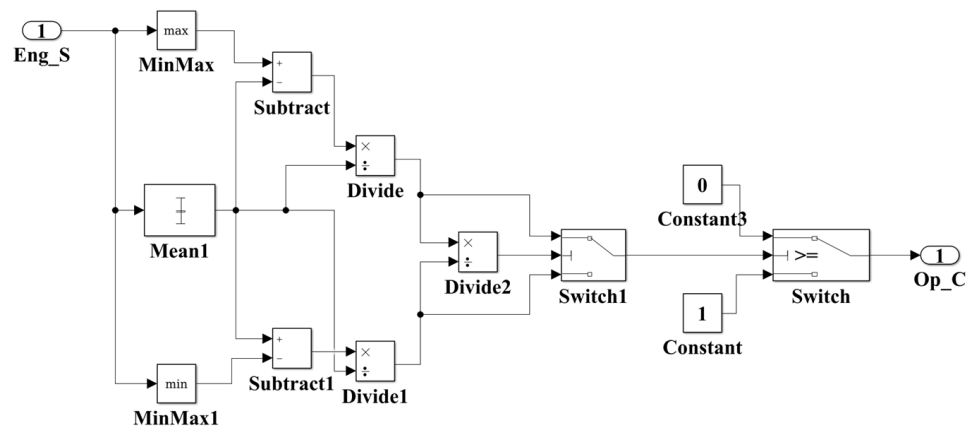


Figure 13. Rotational speed modules.

The exhaust temperature calculation modules are shown in Figure 14. The calculation of the mean and the mean squared deviation values for exhaust gas temperatures, etc. was performed. The difference between the exhaust temperature of each cylinder and the average was calculated to provide data for subsequent judgments.

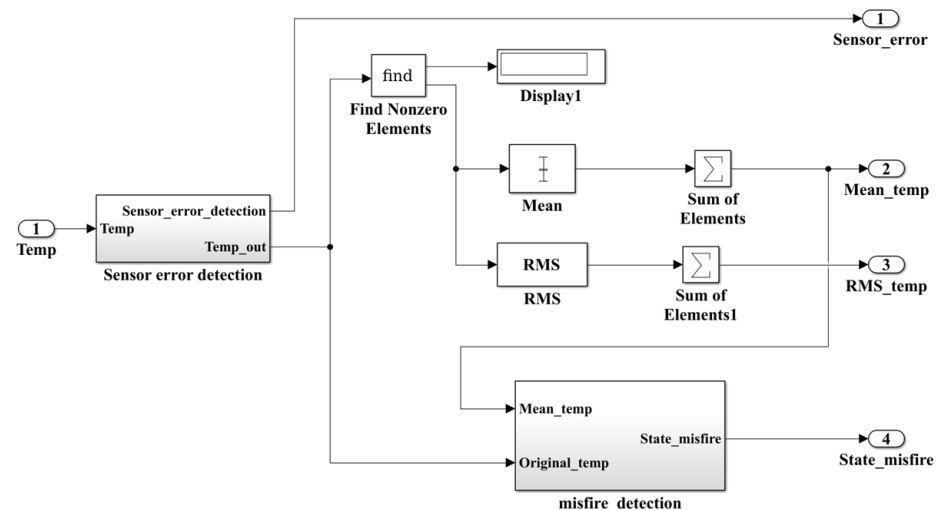


Figure 14. Exhaust temperature calculation modules.

3.3. Misfire Detection and Determination

A misfire is an extreme case of non-uniformity of each cylinder where the exhaust temperature is significantly lower than the normal working cylinder. Numerical analysis of the exhaust temperature shows whether there is a misfire.

The misfiring cylinder was identified. According to the exhaust temperature analysis and calculation results, if the exhaust temperature of a certain cylinder or certain cylinders is significantly lower than that of other cylinders, and the difference with other cylinders exceeds a certain limit, it will be judged as a misfire, and the number of misfired cylinders is greater than a certain limit. When the value is set, it will set off an alarm or even stop; if the multi-cylinder misfire flag is determined as the misfired cylinder, the flag signal will be given, and the misfired cylinder will be shielded and the fuel injection quantity will be set to 0. The misfired cylinder will also be shielded when the non-uniformity of each cylinder is calculated. Other cylinders normally perform fuel quantity compensation.

3.4. Closed-Loop Fuel Quantity Compensation

The exhaust temperature compensation calculation modules are shown in Figure 15. Figure 16 shows the fuel quantity compensation ratio calculation module of each cylinder. According to the base fuel quantity injection pulse spectrum, the fuel quantity compensation of each cylinder was adjusted. A compensation ratio of 1 means that no compensation was made for this cylinder's fuel quantity, 0 means the cylinder did not inject fuel, more than 1 means an increase in the quantity of energy for this cylinder, and more than 0 but less than 1 means the fuel quantity of this cylinder was reduced. The compensation ratio was determined according to the range of the difference between the last exhaust temperature and the average exhaust temperature. A more considerable difference means a more significant discrepancy between the compensation fuel quantity and the base fuel quantity.

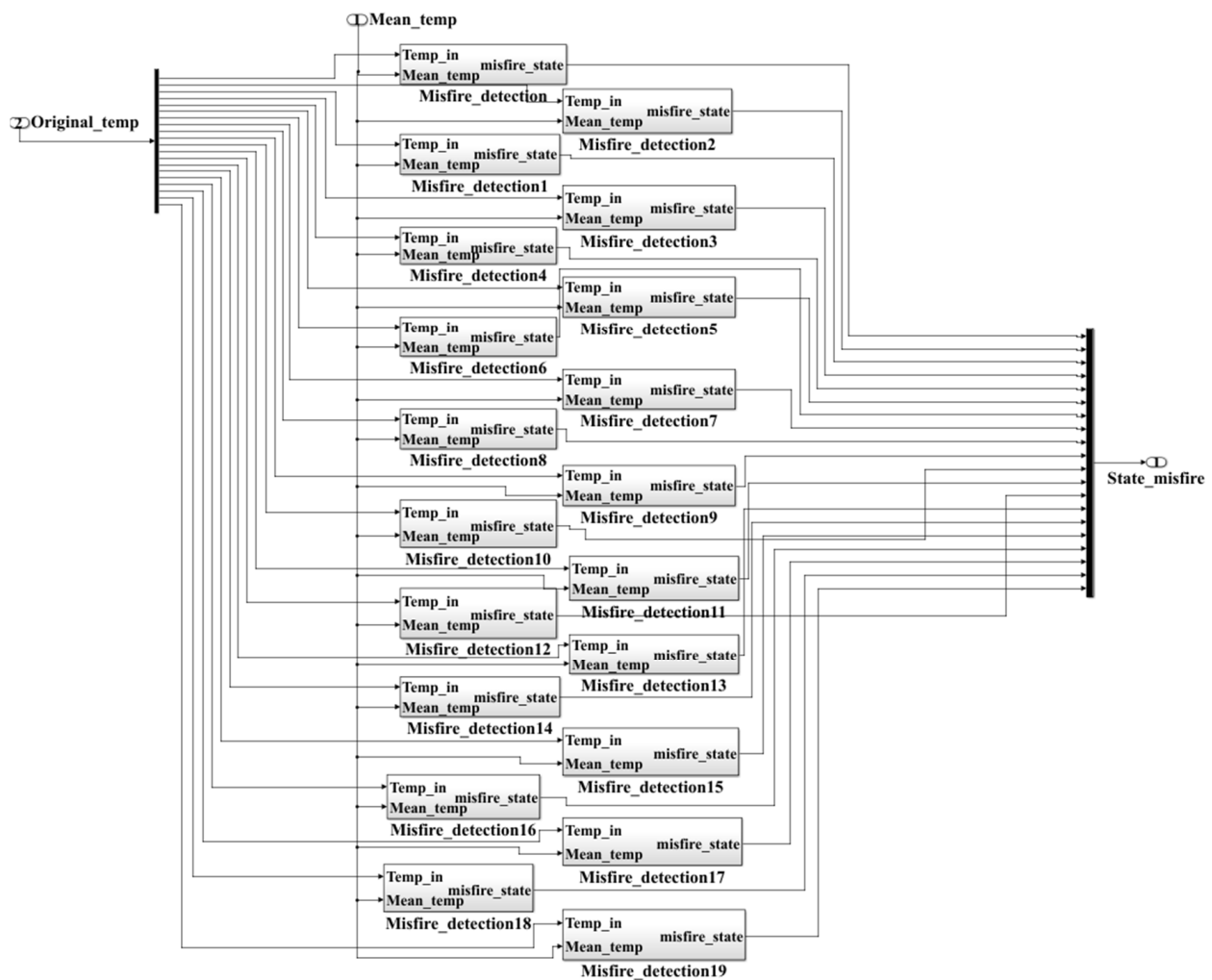


Figure 15. Exhaust temperature compensation calculation modules.

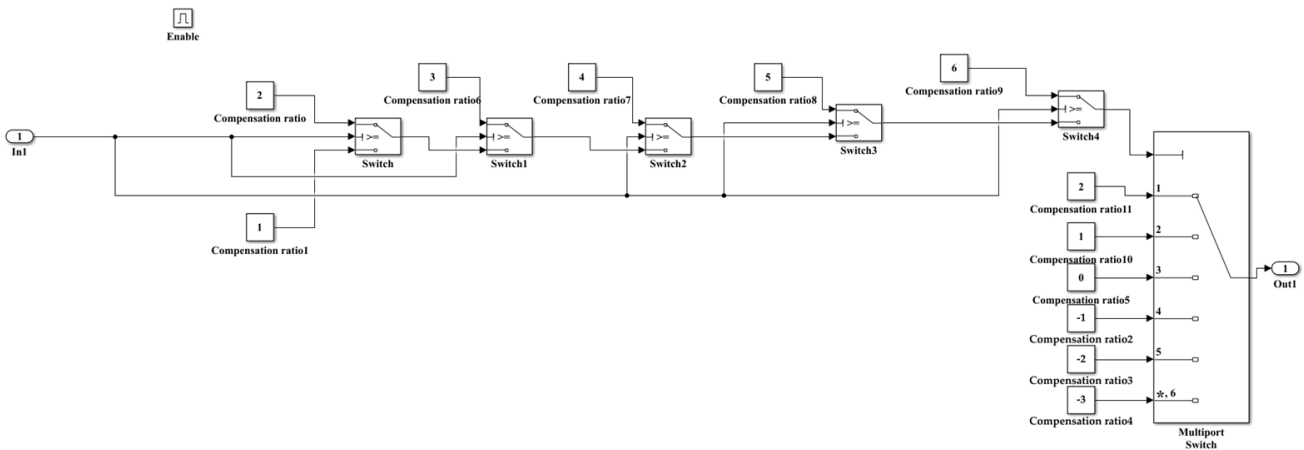


Figure 16. Fuel quantity compensation ratio calculation modules.

Figure 17 shows the flow of fuel compensation and calibration. The fuel compensation count was prepared for identifying the blind spots of the non-uniformity algorithm of each cylinder. When the fuel quantity compensation exceeded the specified frequency and the non-uniformity of each cylinder was not improved in any way, the adjustment of the fuel quantity of each cylinder was stopped. The compensation fuel ratio of 1 represented non-uniformity in each cylinder caused by the fuel injection system.

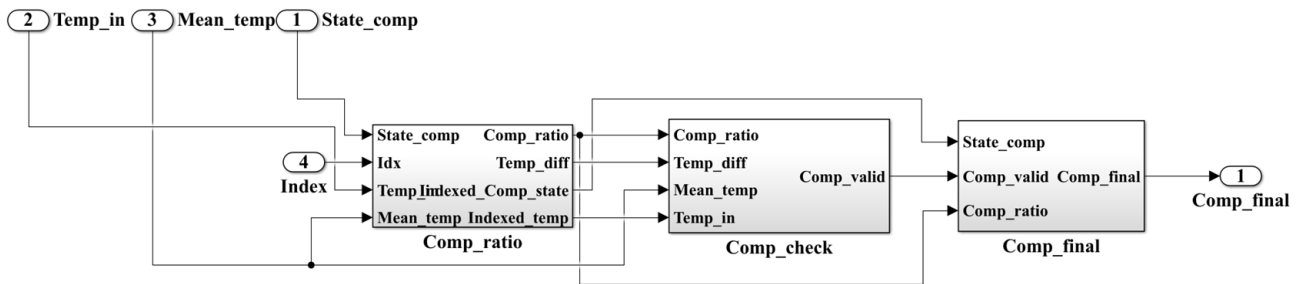


Figure 17. The fuel quantity compensation and calibration process.

In the cycle of progressive split-cylinder fuel compensation, the calculated compensation ratio is larger when the difference between the single-cylinder exhaust temperature and the average exhaust temperature is larger. A large difference in fuel quantity causes speed fluctuation. Progressive fuel compensation is adopted to gradually improve the non-uniformity of each cylinder when the difference is above a specific value.

The abovementioned control strategy was used on the SIMULINK platform for the software in-loop regulation of cylinder non-uniformity in MATLAB R2017a. The information was obtained through the calibration and analysis of the feedback signals. Finally, the non-uniformity of each cylinder due to the fuel injection system was achieved by correcting the injection pulse spectrum.

4. Non-Uniformity Control Co-Simulation

To evaluate the effectiveness of the cylinder exhaust temperature based on the CUC strategy, software-in-the-loop simulations are carried out.

4.1. Simulation Scheme

As shown in Figure 1, the joint simulation of SIMULINK and AVL-Cruise M is based on the compilation of the engine model into a SIMULINK executable Cruise.mdl file using the CMC Interface module in AVL Cruise M. The engine model was loaded into a library of modules in SIMULINK. It was loaded into the module library in SIMULINK and dragged and dropped directly into SIMULINK for direct invocation when building the simulation

control model, which was used to provide objects for subsequent controller development. Figure 18 shows the joint simulation on the SIMULINK platform.

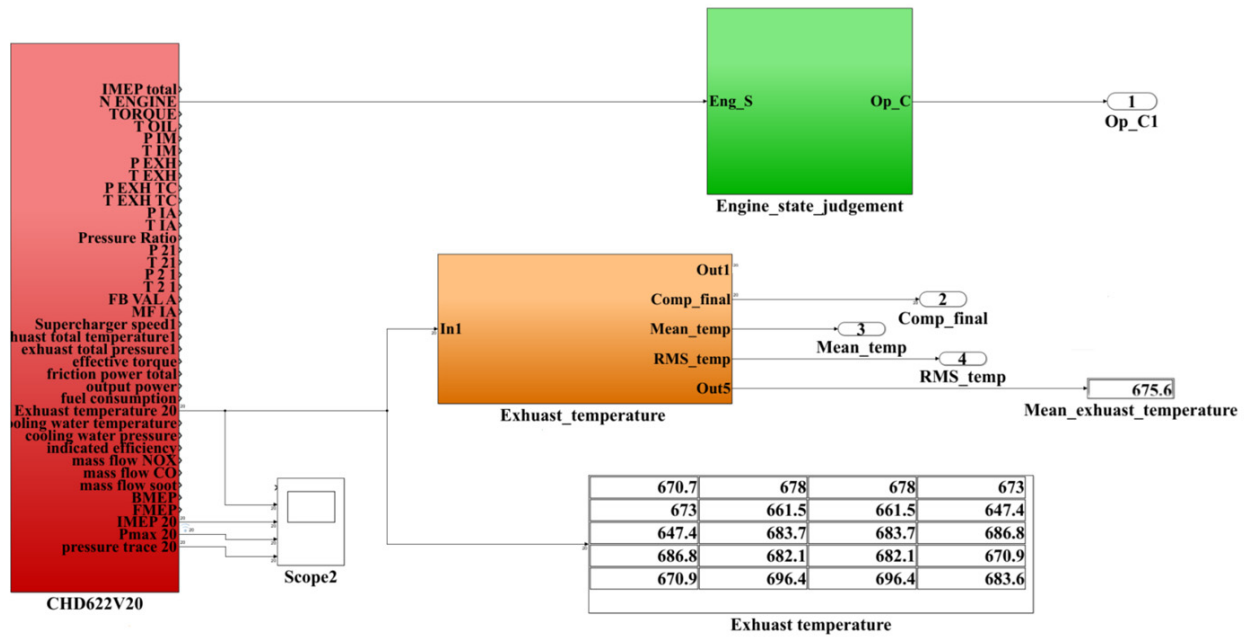


Figure 18. Joint simulation model on the SIMULINK platform.

The input and output interfaces of the real-time model were defined according to the requirements of the control strategy. The model inputs consisted of 125 signals, including the timing and pulse width of the three injections, starting signals, etc. The model outputs consisted of 56 signals, including the engine speed, supercharger speed and pressure, exhaust temperature and pressure of each cylinder, and output power.

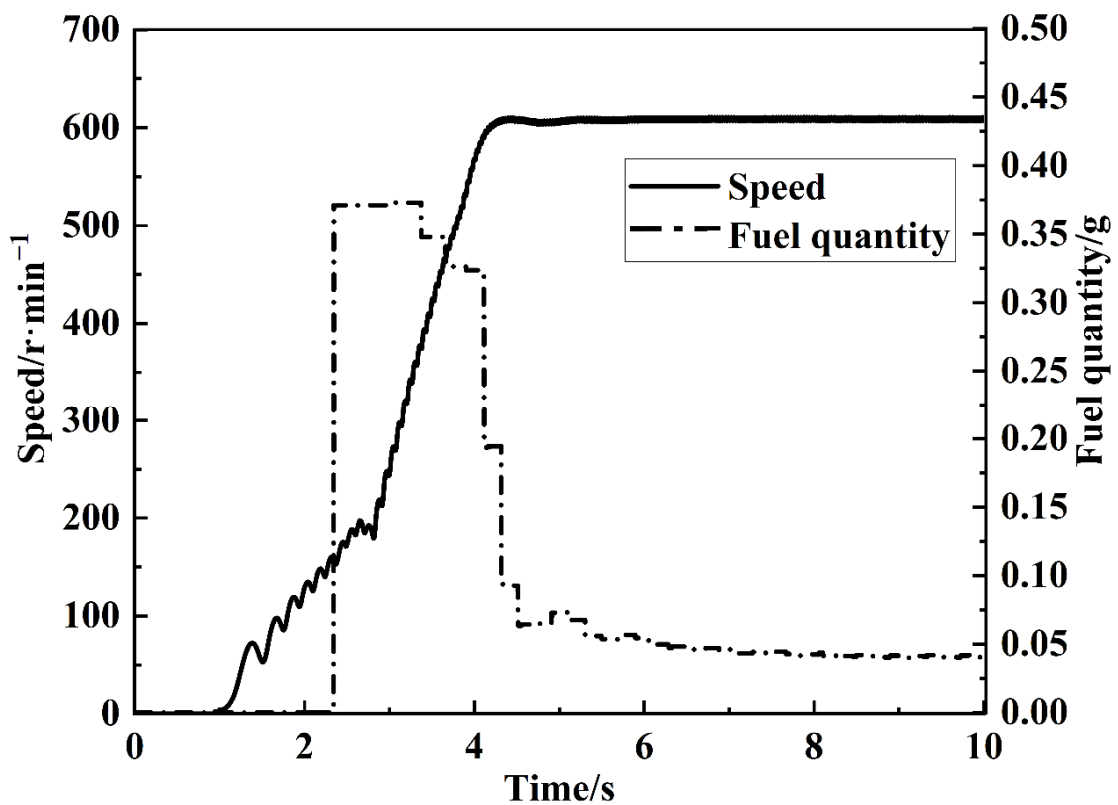
4.2. Verification of the Control Strategy

Figure 19a shows the instantaneous speed and fuel injection curves for the starting and idling conditions. When the speed of the high-speed engine reached 150 r/min, the injector started to inject fuel; when the speed reached 600 r/min, the starting process ended and the idling condition began. Additionally, the transition from the starting condition to the idling condition was smooth, and the fluctuation rate of speed under the idling condition was less than 1%, thereby meeting the secondary accuracy requirements of speed regulation.

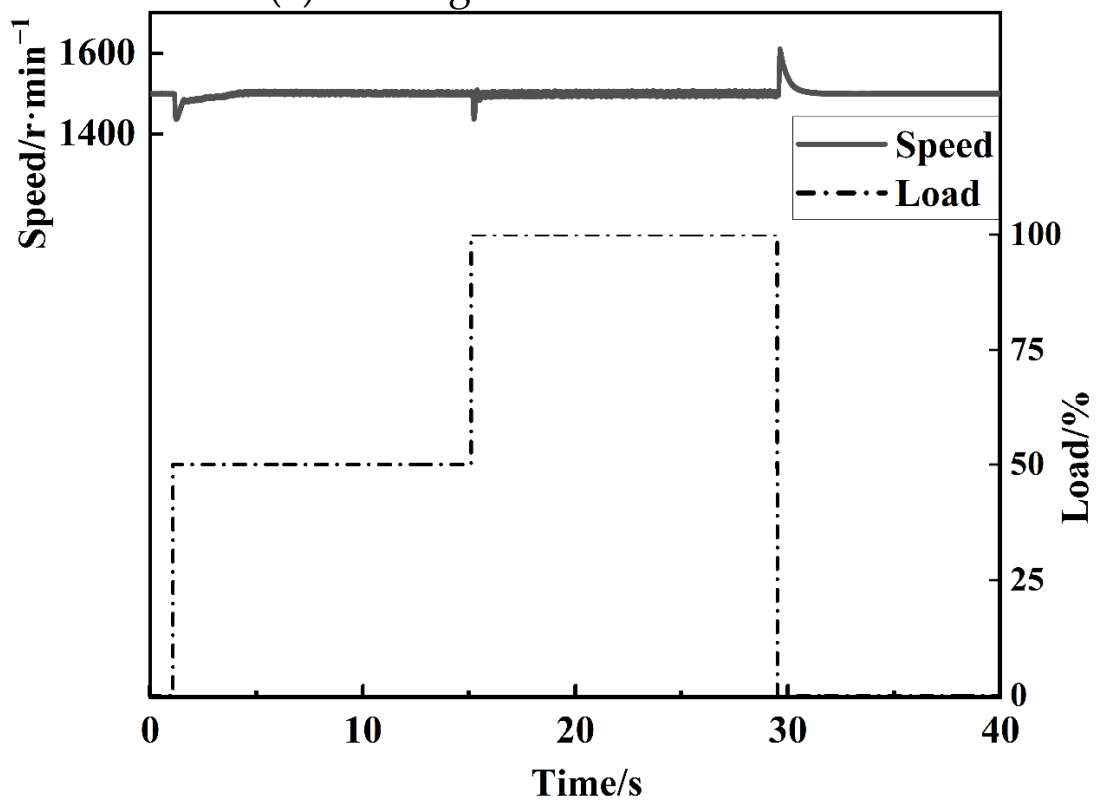
Figure 19b shows that the speed of the high-speed engine was stable at 1500 r/min; after experiencing a sudden load reduction, the speed could still be stabilized at 1500 r/min, and the steady-state speed regulation, transient speed regulation, and stabilization time all met the requirements of the classification society for speed control.

4.3. Software-In-The-Loop Simulation Results

To compare the effects of the non-uniformity control strategy based on the exhaust temperature of each cylinder and the control strategy based on the cylinder pressure, a comparison was performed in the software in-loop, as shown in Figure 20; the high-speed engine was under the calibrated speed and 100% load. The comparison charts of IMEP, P_{max} (the maximum burst pressure), and T_{ex} are shown in the figure.



(a) Starting and idle conditions



(b) Sudden loading and load reduction at rated speed

Figure 19. Basic control function verification.

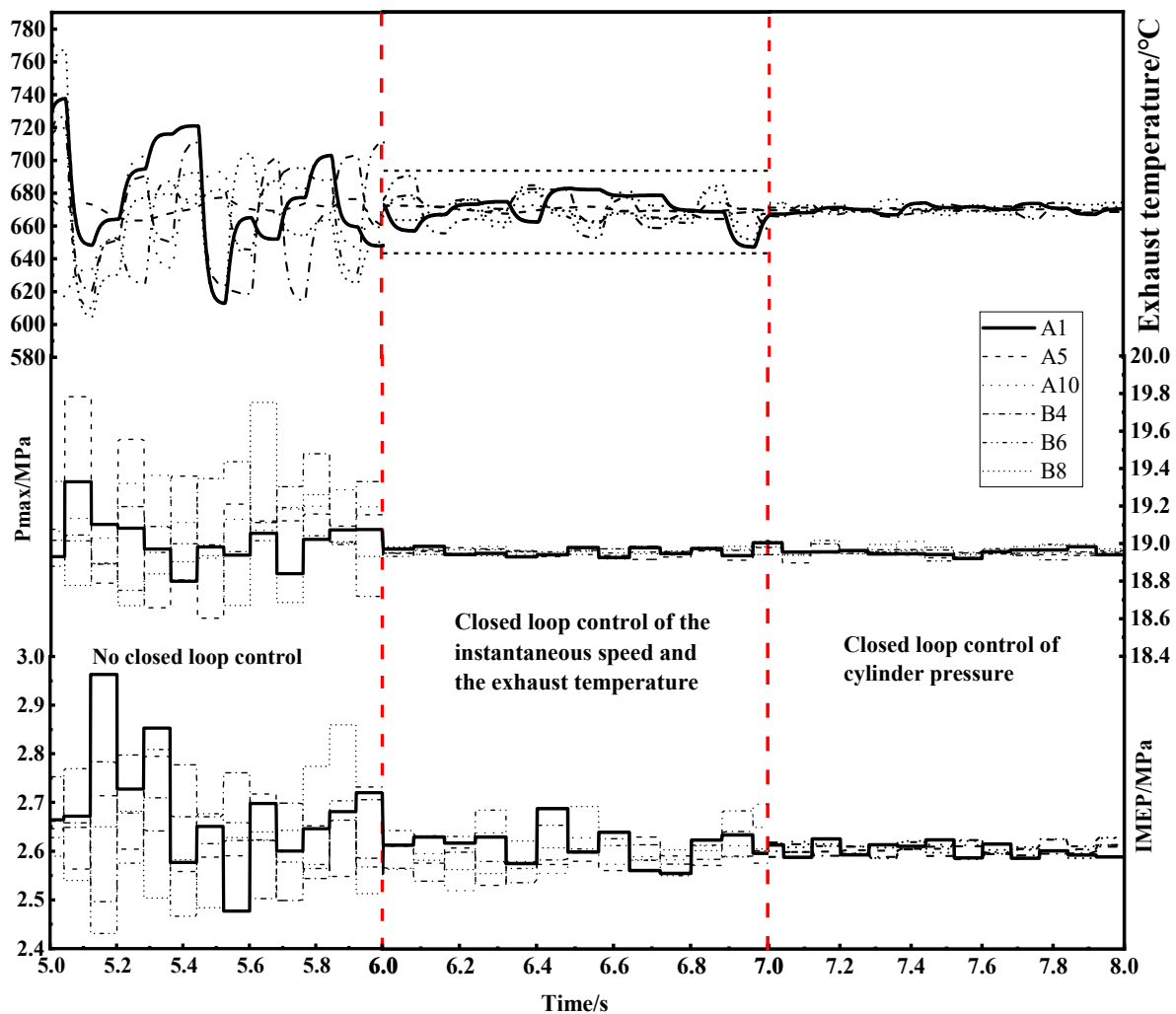


Figure 20. Comparison of the two control modes: IMEP and P_{max} and T_{ex} at 100% load.

IMEP provides a direct indication of the dynamics and economy of combustion, so controlling IMEP reduces the non-uniformity of the work performed by each cylinder [29], and IMEP reduces the effect of random errors and has high data reliability. P_{max} indicates the maximum value of cylinder pressure within an operating cycle. P_{max} directly reflects the maximum mechanical shock that the engine is subjected to in the current cycle, and is also an important indicator of abnormal in-cylinder combustion [28].

The CV of IMEP, P_{max} and T_{ex} were selected as the index of the in-cylinder combustion inhomogeneity. Cylinders A1, A5, A10, B4, B6, and B8 were selected for demonstration in the figure. The indicators IMEP, P_{max} and T_{ex} were compared under no closed-loop control, closed-loop control based on the exhaust temperature of each cylinder, and closed-loop control based on the cylinder pressure. The dispersion of IMEP and P_{max} for each cylinder was significantly smaller for the high-speed engine when operating in the exhaust temperature inhomogeneity control and cylinder pressure control modes compared with the no closed-loop control. The non-uniformity of each cylinder was significantly improved under both closed-loop controls.

Figure 21 shows a comparison of the CV of the combustion characteristic parameters when the high-speed engine was operated under different loads using closed-loop speed exhaust temperature control and closed-loop cylinder pressure control, respectively. At each load, the CV of IMEP and P_{max} for each cylinder was reduced by approximately 99% for both methods, although the use of closed-loop cylinder pressure control reduced the coefficient of variation of IMEP and P_{max} for each cylinder slightly more significantly than

closed-loop speed and exhaust temperature control, which makes closed-loop speed and exhaust temperature control more feasible when considering the cost of sensors. With the closed-loop control of exhaust temperature and instantaneous speed, the CV of T_{ex} was close to the closed-loop control of cylinder pressure; the maximum error occurred at 25% load, when was 0.114%. The CV of IMEP was close to the closed-loop control of cylinder pressure; the maximum occurred at 25% load, when it is 0.199%. The CV of P_{max} was close to the closed-loop control of cylinder pressure up to 0.025% at 100% load.

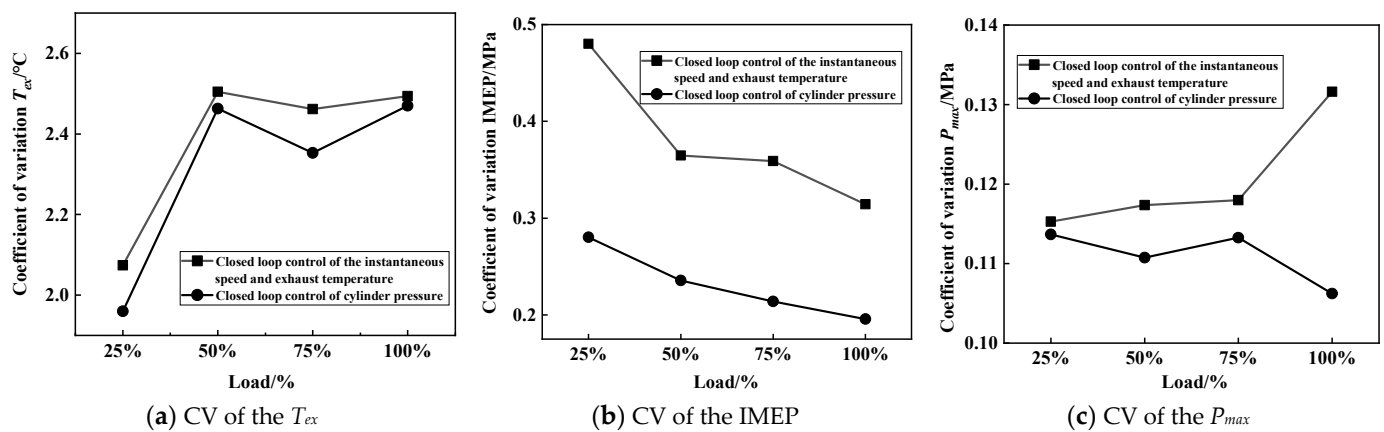


Figure 21. Coefficients of the combustion characteristic parameters of the two closed-loop controls.

5. Conclusions

The CHD622V20 marine high-speed engine was studied and a real-time simulation model was established in AVL Cruise M. A CUC strategy based on the instantaneous speed and exhaust temperature of each cylinder was developed in SIMULINK, and the marine high-speed engine model was integrated in the loop. The CUC of the marine high-speed diesel engine was investigated and compared with the cylinder-pressure-based control strategy to provide a theoretical basis for subsequent hardware-in-the-loop and tests.

- (1) For multi-cylinder marine diesel engines, after the closed-loop control, the inhomogeneity of each cylinder caused by the fuel injection system was significantly improved. Although the control effect of using the exhaust temperature of each cylinder as the feedback variable for the marine high-speed engine was not as outstanding as that of using cylinder pressure, it did not require additional expensive cylinder pressure sensors, which significantly reduced the cost and provided better reliability and feasibility;
- (2) With the closed-loop control of exhaust temperature and instantaneous speed, the CV of IMEP was close to the closed-loop control of cylinder pressure, and the maximum occurred at 25% load, when it was 0.199%. The CV of P_{max} was close to the closed-loop control of cylinder pressure up to 0.025% at 100% load. The CV of T_{ex} was close to the closed-loop control of cylinder pressure, and the maximum occurred at 25% load, when it was 0.114%.
- (3) This platform was used to study the effect of the control strategy on the uniformity of each cylinder and the overall performance of the marine high-speed diesel engine and provide a theoretical basis for the subsequent hardware-in-the-loop simulation and actual engine tests.

Author Contributions: Conceptualization, L.X.; methodology, L.X.; software, L.X. and S.S.; validation, L.X. and F.D.; writing—original draft preparation, L.X. All authors have read and agreed to the published version of the manuscript.

Funding: This research received no external funding.

Data Availability Statement: All data generated or analyzed during this study are included in this published article.

Acknowledgments: The authors would like to thank the editor in chief, associate editor and the anonymous referees for detailed and valuable comments that helped to improve this manuscript.

Conflicts of Interest: The authors declare no conflict of interest.

Nomenclature

Symbols

AF_{ST}	the stoichiometric air-fuel ratio
A_{NS}	the flow cross-sectional area of the needle valve seat
A_{NH}	the flow cross-sectional area of the nozzle
A_i	the surface area of the thermal system boundary
α_w	the heat transfer coefficient
C_{pre}	the premixed combustion exothermic calibration parameter
C_{comb}	the calibrated experimentally and related to speed
dm_i	the quality of the air flowing into the cylinder
dm_e	the quality of the exhaust gas flowing
dm_{pump}	the fuel mass supplied to the high-pressure oil pump
dm_{inj}	the fuel mass supplied to the common rail injector
dQ_s/dt	the heat lost by the compressed air
dQ_w/dt	the heat gained by the coolant
dQ_{sw}/dt	the heat transferred from the compressed air to the coolant
E	the volume elastic modulus of the fuel
F_{wall}	the function of wall effects during fuel injection
F_{egr}	the function of residual gas effects
h_i	the inflow enthalpy
h_e	the outflow enthalpy
H_u	the low heating value of the fuel
k	the turbulent kinetic energy intensity
m_c	the quality of the working substance in the cylinder
$m_{f,pre}$	the fuel mass in the premixed
$m_{f,diff,net}$	the fuel mass during the diffusion combustion
P_c	the pressure in the cylinder
P_{max}	the maximum burst pressure
P_{rail}	the pressure in the common rail
P_{pipe}	the pressure in the high-pressure oil pipe
Q_w	the heat transfer rate
Q_{wi}	the heat between the working substance and the thermal system boundary
Q_{pre}	the heat in the premixed combustion
Q_{diff}	the heat in the diffusion combustion
$t-t_{ign}$	the length of time since fuel ignition
T_{ex}	the exhaust temperature
T_c	the working substance temperature in the cylinder
T_{wi}	the temperature of the thermal system boundary
T_{wo}	the temperature of the coolant after the intercooler
T_{in}	the in-cylinder temperature
T_K	the temperature of the air before the intercooler
T_S	the temperature of the air after the intercooler
u	the ratio of the internal energy
V_{mix}	the fuel injection volume
V_c	the cylinder volume
V_{rail}	the volume of the common rail
κ and T_A	the Arrhenius exothermic model constants
ρ_{rail}	the volume of the fuel in the common rail

ρ_{fuel}	the density of fuel
ξ_{NS}	the flow coefficient of the needle valve seat
ξ_{NH}	the flow coefficient of the nozzle hole
λ	the excess air coefficient

Acronyms

CV	Coefficient of variation
IMEP	Indicated effective pressure
HPCR	High pressure common rail
TDC	Top dead center
CUC	Cylinder uniformity control
MFB50	50% of the mass fraction burned
MCC	Mixing controlled combustion
CPU	Central processing unit

References

- Ding, S.; Yang, L.; Song, E. *Investigations on In-Cylinder Pressure Cycle-to-Cycle Variations in a Diesel Engine by Recurrence Analysis*; SAE Technical Paper 2015-01-0875; SAE International: Warrendale, PA, USA, 2015.
- Hoang, A.T.; Foley, A.M.; Nižetić, S.; Huang, Z.H.; Ong, H.C.; Ölçer, A.I.; Pham, V.V.; Nguyen, X.P. Energy-related approach for reduction of CO₂ emissions: A critical strategy on the port-to-ship pathway. *J. Clean. Prod.* **2022**, *355*, 131772. [[CrossRef](#)]
- Hoang, A.T.; Tran, V.D.; Dong, V.H.; Le, A.T. An experimental analysis on physical properties and spray characteristics of an ultrasound-assisted emulsion of ultra-low-sulphur diesel and Jatropa-based biodiesel. *J. Mar. Eng. Technol.* **2022**, *21*, 73–81. [[CrossRef](#)]
- Xu, N.; Zhang, G.L.; Yang, L.B.; Shen, Z.Y.; Xu, M.; Chang, L. Research on thermoeconomic fault diagnosis for marine low speed two stroke diesel engine. *Math. Biosci. Eng.* **2022**, *19*, 5393–5408. [[CrossRef](#)] [[PubMed](#)]
- Wang, Y.H.; Wang, G.Y.; Yao, G.Z.; Shen, L.Z. Research on the Characteristics of Operating Non-Uniformity of a High-Pressure Common-Rail Diesel Engine Based on Crankshaft Segment Signals. *IEEE Access* **2021**, *9*, 64906–64917. [[CrossRef](#)]
- Carlos, G.; Benjamín, P.; Pau, B.; Alvin, B. Closed-loop control of a dual-fuel engine working with different combustion modes using in-cylinder pressure feedback. *Int. J. Engine Res.* **2020**, *21*, 484–496.
- Zhu, Y.Q.; Li, T.H.; Xia, C.; Feng, Y.M.; Zhou, S. Simulation analysis on vaporizer/mixer performance of the high-pressure SCR system in a marine diesel. *Chem. Eng. Process.* **2020**, *148*, 107819. [[CrossRef](#)]
- Ju, D.H.; Jia, X.X.; Huang, Z.; Qiao, X.Q.; Xiao, J.; Huang, Z. Comparison of atomization characteristics of model exhaust gas dissolved diesel and gasoline. *Fuel* **2016**, *182*, 928–934. [[CrossRef](#)]
- Zhou, F.; Fu, J.Q.; Shu, J.; Liu, J.P.; Wang, S.Q.; Feng, R.H. Numerical simulation coupling with experimental study on the non-uniform of each cylinder gas exchange and working processes of a multi-cylinder gasoline engine under transient conditions. *Energy Convers. Manag.* **2016**, *123*, 104–115. [[CrossRef](#)]
- Zhong, Y.H.; Zhang, Y.H.; Mao, C.F.; Ananchai, U. Performance, Combustion, and Emission Comparisons of a High-Speed Diesel Engine Fueled with Biodiesel with Different Ethanol Addition Ratios Based on a Combined Kinetic Mechanism. *Processes* **2022**, *10*, 1689. [[CrossRef](#)]
- Zhou, X.Y.; Tie, L.; Wang, N.; Wang, X.R.; Chen, R.; Li, S.Y. Pilot diesel-ignited ammonia dual fuel low-speed marine engines: A comparative analysis of ammonia premixed and high-pressure spray combustion modes with CFD simulation. *Renew. Sustain. Energy Rev.* **2023**, *173*, 113108. [[CrossRef](#)]
- Kalen, R.V.; Gregory, M.S.; Mrunal, C.J.; James, M. Implementing variable valve actuation on a diesel engine at high-speed idle operation for improved aftertreatment warm-up. *Int. J. Engine Res.* **2020**, *21*, 1134–1146.
- Wang, Y.H.; Wang, G.Y.; Yao, G.Z.; Shen, L.Z. Research on Fuel Offset Control of High-Pressure Common-Rail Diesel Engine Based on Crankshaft Segment Signals. *Sens.* **2022**, *22*, 3355. [[CrossRef](#)]
- Yun, H.; Kang, J.; Chang, M.; Najt, P. *Improvement on Cylinder-to-Cylinder Variation Using a Cylinder Balancing Control Strategy in Gasoline HCCI Engines*; SAE Technical Paper 2010-01-0848; SAE International: Warrendale, PA, USA, 2010.
- Shen, Z.J.; Cui, W.Z.; Liu, Z.C.; Tian, J. Distribution evolution of intake and residual gas species during CO₂ stratification combustion in diesel engine. *Fuel* **2016**, *166*, 427–435. [[CrossRef](#)]
- Ott, T.; Zurbriggen, F.; Onder, C.; Guzzella, L. Cylinder individual feedback control of combustion in a dual fuel engine. *IFAC Proc.* **2013**, *46*, 600–605. [[CrossRef](#)]
- Zheng, X.Q.; Yang, J.G.; Huang, L.F.; Zhu, S.L. Experimental Research of Cylinder Balance Control for a Marine Micro-Pilot-Ignition Dual-Fuel Engine. *Trans. CSICE* **2021**, *39*, 51–60.
- Ou, S.H.; Yu, Y.H.; Yang, J.G. Identification and reconstruction of anomalous sensing data for combustion analysis of marine diesel engines. *Meas.* **2022**, *193*, 110960. [[CrossRef](#)]
- Yu, Y.H.; Shen, Y.L.; Wang, Q.P.; Yang, J.G. Research on Hardware-in-Loop Simulation Technology of In-Cylinder Pressure Closed-Loop Control for Low-Speed Marine Diesel Engines. *Chin. Intern. Combust. Engine Eng.* **2019**, *40*, 86–92.
- Kazienko, D.; Chybowski, L. Instantaneous Rotational Speed Algorithm for Locating Malfunctions in Marine Diesel Engines. *Energies* **2020**, *13*, 1396. [[CrossRef](#)]

21. Yang, J.G. Fault detection in a diesel engine by analyzing the instantaneous angular speed. *Mech. Syst. Signal Process.* **2001**, *15*, 549–564. [[CrossRef](#)]
22. Kim, H.J.; Park, S.H.; Lee, C.S. Impact of fuel spray angles and injection timing on the combustion and emission characteristics of a high-speed diesel engine. *Energy* **2016**, *107*, 572–579. [[CrossRef](#)]
23. Katersnik, T.; Lund, H.; Kaiser, M.J. An advanced real-time capable mixture-controlled combustion model. *Energy* **2016**, *95*, 393–403. [[CrossRef](#)]
24. Kim, K.S.; Ghandhi, J. *A Simple Model of Cyclic Variation*; SAE Technical Paper 2012-32-0003; SAE International: Warrendale, PA, USA, 2012.
25. Marsaglia, G.; Bray, T.A. A Convenient Method for Generating Normal Variables. *Siam Rev.* **1964**, *6*, 260–264. [[CrossRef](#)]
26. Alexander, W.; Rolf, I. Semi-physical state and parameter estimation of diesel combustion phases for real-time applications. *Int. J. Engine Res.* **2020**, *21*, 1800–1818.
27. Chen, Z.F.; Yao, C.D.; Wang, Q.G.; Han, G.P.; Dou, Z.C.; Wei, H.Y.; Wang, B.; Liu, M.J.; Wu, T.Y. Study of cylinder-to-cylinder variation in a diesel engine fueled with diesel/methanol dual fuel. *Fuel* **2016**, *170*, 67–76. [[CrossRef](#)]
28. Chung, J.; Min, K.; Oh, S.; Sunwoo, M. In-cylinder pressure based real-time combustion control for reduction of combustion dispersions in light-duty diesel engines. *Appl. Therm. Eng.* **2016**, *99*, 1183–1189. [[CrossRef](#)]
29. Zhang, Y.H.; Shen, T.L. Cylinder pressure-based combustion phase optimization and control in spark-ignited engines. *Control. Theory Technol.* **2017**, *15*, 83–91. [[CrossRef](#)]

Disclaimer/Publisher’s Note: The statements, opinions and data contained in all publications are solely those of the individual author(s) and contributor(s) and not of MDPI and/or the editor(s). MDPI and/or the editor(s) disclaim responsibility for any injury to people or property resulting from any ideas, methods, instructions or products referred to in the content.